Optical Engineering

OpticalEngineering.SPIEDigitalLibrary.org

Deflection angle detecting system for the large-angle and high-linearity fast steering mirror using quadrant detector

Yingxue Ni
Jiabin Wu
Xiaogang San
Shijie Gao
Shaohang Ding
Jing Wang
Tao Wang

SPIE.

Yingxue Ni, Jiabin Wu, Xiaogang San, Shijie Gao, Shaohang Ding, Jing Wang, Tao Wang, "Deflection angle detecting system for the large-angle and high-linearity fast steering mirror using quadrant detector," *Opt. Eng.* **57**(2), 024110 (2018), doi: 10.1117/1.OE.57.2.024110.

Optical Engineering 57(2), 024110 (February 2018)

Deflection angle detecting system for the large-angle and high-linearity fast steering mirror using quadrant detector

Yingxue Ni,[a,b] Jiabin Wu,[a,*] Xiaogang San,[a] Shijie Gao,[a] Shaohang Ding,[a,b] Jing Wang,[a] and Tao Wang[a,b]
[a]Changchun Institute of Optics, Fine Mechanics and Physics, Changchun, China
[b]University of Chinese Academy of Sciences, Beijing, China

Abstract. A deflection angle detecting system (DADS) using a quadrant detector (QD) is developed to achieve the large deflection angle and high linearity for the fast steering mirror (FSM). The mathematical model of the DADS is established by analyzing the principle of position detecting and error characteristics of the QD. Based on this mathematical model, the method of optimizing deflection angle and linearity of FSM is demonstrated, which is proved feasible by simulation and experimental results. Finally, a QD-based FSM is designed and tested. The results show that it achieves 0.72% nonlinearity, ± 2.0 deg deflection angle, and 1.11-μrad resolution. Therefore, the application of this method will be beneficial to design the FSM. [DOI: 10.1117/1.OE.57.2.024110]

Keywords: angle detecting system; fast steering mirror; quadrant detector; high linearity; large deflection angle.

Paper 171184 received Jul. 28, 2017; accepted for publication Jan. 30, 2018; published online Feb. 26, 2018.

1 Introduction

On the free-space optical communication (FSO) links, the light beam may deviate from the terminal due to the external mechanical and atmospheric disturbances, causing bit error rate to increase and even communication outage.[1–3] Thus, it is very necessary to accurately control the transmission direction of light beam. As a device capable of steering light beam fast and precisely, the fast steering mirror (FSM) has been applied to the acquisition, pointing, and tracking (APT) of an FSO system.[4–6] In addition, it has also been widely applied to some other fields, such as lidar, astronomical telescope, and image stabilization.[7–9]

With the tendency of extending the acquisition field and improving tracking precision of the APT system, the FSM with large deflection angle and high linearity has recently become a research focus.[10–12] The deflection angle of FSM can be detected by the position sensor which also provides angle feedback for actuators. Its performance directly affects the deflection angle and linearity of the FSM. Generally, there are several kinds of FSMs using different position sensors such as a capacitance probe sensor, eddy current proximity sensor as well as electro-optic sensors [such as position-sensitive detectors (PSD) and quadrant detectors (QD)].[4] Researchers have done many studies about FSMs driven by voice coil actuators (VCA) and also made some noticeable results. A kind of FSM provided by OIM, using eddy current proximity sensor, achieves ± 1.5 deg deflection angle and 1% nonlinearity.[13] Lu et al.[14] reported an FSM based on a capacitance probe sensor, which achieves ± 5 deg along two axes. Wu et al.[8] introduced a PSD-based FSM, which has ± 1.125 deg and ± 2.5 deg deflection angle in x-axis and y-axis, respectively, and 2.6% nonlinearity.

The studies show that the capacitance probe sensor has a relatively small measurement range. The eddy current proximity sensor takes too much space, because the ideal target size is three times the sensor radius (such as MICRO-EPSILON NCTD3300).[8,15,16] Both the PSD and QD can be used to detect the deflection angle for the large-angle FSM. In addition, the QD has better linearity and faster response than the PSD,[17–19] which is widely applied to many equipments to detect the deflection angle. Therefore, the QD is more suitable for the FSM to achieve larger deflection angle and better linearity.

In this paper, a QD-based deflection angle detecting system (DADS) is designed in detail for FSM, according to the principle of specular reflectivity. Its mathematical model is established by analyzing the principle of position detecting and error characteristics of the QD. We can optimize the deflection angle and the linearity of the FSM by changing the parameters of the DADS according to the mathematical model. This optimization method is verified by lots of simulations and experiments. In addition, we design the QD-based FSM and test its performances such as deflection angle, linearity, and resolution. The results show that the method of optimizing the deflection angle and linearity for DADS will be beneficial for improving the performances of FSM.

This paper is organized as follows: in Sec. 2, the working principle of the DADS is introduced. In Sec. 3, the mathematical model of the DADS is established, and the method of optimizing deflection angle and linearity of FSM is studied. Section 4 describes a series of experiments of the DADS and the QD-based FSM.

2 Principle of the Deflection Angle Detecting System

2.1 *Fast Steering Mirror Structure*

The exploded view of the FSM is shown in Fig. 1. It is mainly composed of the major mirror, flexible hinge support, four voice coil actuators (VCAs), main casing, and the

*Address all correspondence to: Jiabin Wu, E-mail: wujiabin777@163.com

0091-3286/2018/$25.00 © 2018 SPIE

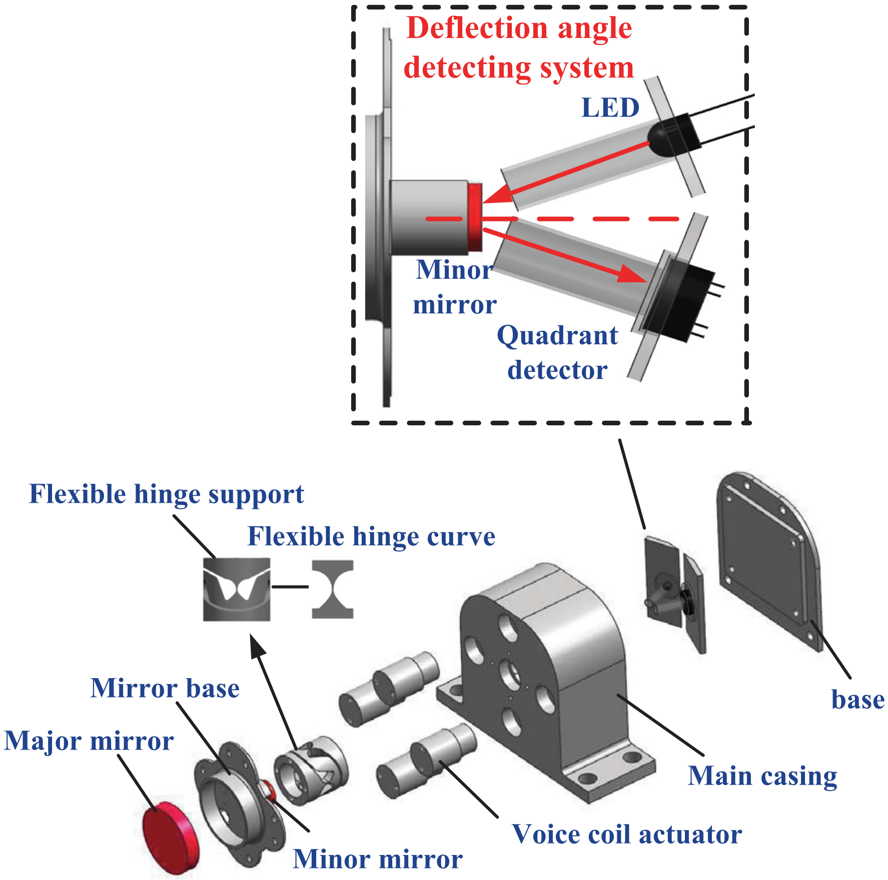

Fig. 1 Exploded the view of the QD-based FSM.

DADS. The major mirror is stuck to the mirror base supported by flexible hinge, which is fixed in the front of the main casing with screws. The magnets of VCAs are mounted on the back of the mirror base, and the coils are fixed on the main casing. Two pairs of VCAs mounted perpendicularly drive the FSM to deflect via elastic deformation of the flexible hinge. The deflection angle is detected by the DADS, which is composed of the QD, LED, and minor mirror. The beam emitted from the light source is reflected by the minor mirror, then arrives at the QD, which is used to detect angle information of the minor mirror. LED and QD are mounted symmetrically about the normal of the minor mirror. The minor mirror is stuck on the back of the mirror base, and it is in parallel with the major mirror, so the deflection angle of the minor mirror is the same as that of the major mirror; for this reason, the QD can be used to detect the deflection angle of the major mirror.

2.2 *Working Principle of the Quadrant Detector*

Figure 2(a) shows a QD illuminated by an incident Gaussian beam. The QD comprises four identical $p-n$ junction photodiodes separated by the small gaps. With the spot moving on the QD, the position of the spot is estimated according to the voltages generated on each photodiode. The spot position estimation formulas are given as

$$\begin{cases} \sigma_X = \psi_K \frac{U_A+U_C-U_B-U_D}{U_A+U_B+U_C+U_D} \\ \sigma_Y = \psi_K \frac{U_A+U_B-U_C-U_D}{U_A+U_B+U_C+U_D} \end{cases}, \tag{1}$$

where U_A, U_B, U_C, and U_D are the voltages generated on each photodiode, respectively. σ_x and σ_y are the output signal offsets. ψ_k is the proportional coefficient, its value is related to the spot diameter and energy distribution of the spot.[20,21] Generally, there is high linearity of output position only when the spot is near the QD center, and linearity becomes worse gradually with the spot being far from QD center.[22] The spot position measurement error is defined as $\Delta E_{Lx} = x_0 - \sigma_x$, $\Delta E_{Ly} = y_0 - \sigma_y$, where (x_0, y_0) is the theoretical position of the spot center and (σ_x, σ_y) is the estimated position. From Fig. 2(b), it can be seen that there is a maximal positional error in a certain measurement range. The nonlinearity of detecting the spot position using QD in x-axis is defined as

$$\delta_x = |\Delta E_{L\ \max}|/S, \tag{2}$$

where $|\Delta E_{\mathrm{L\ max}}|$ denotes the maximum position measurement error, which is obtained within the measurement range (S).

When the spot is moving on the QD, the performances of the QD in the two axes are symmetrical, all the following discussions are concentrated on the x-axis for simplification.

In addition, the measurement range varies with the spot radius if the value of nonlinearity is fixed, the equation of the relationship between the measurement range and the spot radius is given as[23,24]

$$S = a\omega - b, \tag{3}$$

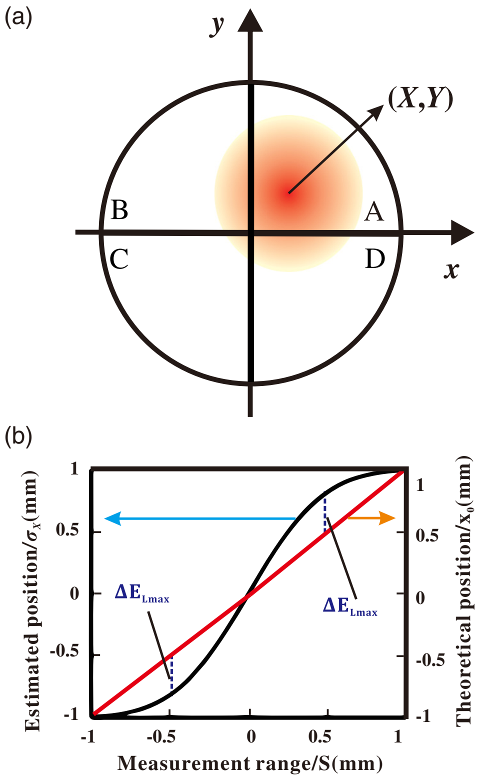

Fig. 2 (a). The incident spot on the QD. (b) The simulation curves of spot position in the measurement range from −1 to 1 mm, the red line represents the theoretical spot position, the black curve is the estimated spot position by simulation.

where a and b are the fitting coefficients, ω is the spot radius. Different nonlinearities correspond to different groups of (a, b). We have also acquired conclusion that the nonlinearity is smaller, the values of a and b are smaller, and the smaller measurement range satisfies the corresponding nonlinearity.

3 Optimization for the Deflection Angle Detecting System

3.1 *Theoretical Research*

Figure 3 shows the working principle of the DADS, and the parameters and symbols are shown in Table 1. When a Gaussian beam impinges on the QD, with the minor mirror deflecting an angle (α), we can obtain the deflection angle of the beam ($\beta = 2\alpha$) based on the geometrical optics theory.

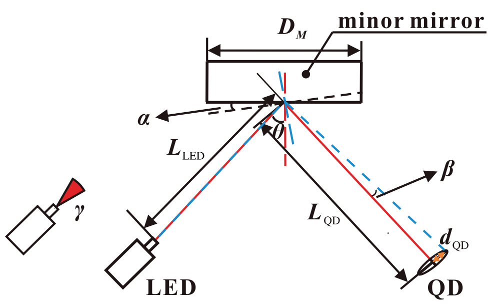

Fig. 3 Work principle diagram of the DADS.

Table 1 Parameters of the DADS.

Symbol	Parameter
D_M	The diameter of the minor mirror
γ	Divergence angle of the LED
α	Absolute value of deflection angle of the minor mirror
θ	The angle between the beam emitted from the LED and normal of the minor mirror
β	Deflection angle of the beam reflected from minor mirror
L_{LED}	The distance between LED and minor mirror
L_{QD}	The distance between minor mirror and the QD
d_{QD}	Range of the spot center moving on the QD

At the same time, the range of spot moving on the QD is given as

$$d_{\text{QD}} = L_{\text{QD}} * \tan 2\alpha, \tag{4}$$

where d_{QD} is the range of the spot center moving on the QD, L_{QD} is the distance between the minor mirror and the QD.

For a certain size of the QD, the relationship between nonlinearity and corresponding measurement range has been analyzed in Sec. 2.2. To achieve small nonlinearity of FSM system, the displacement of spot center on the QD should be no larger than the measurement range of the QD

$$d_{\text{QD}} \leq S. \tag{5}$$

In addition, the incident spot radius on minor the mirror is $L_{\text{LED}} \times \tan \gamma$. To ensure the integrity of the spot illuminating on the minor mirror, the diameter of the minor mirror (D_M) should be bigger than that of the spot ($D_M \geq L_{\text{LED}} \times \tan \gamma$). The spot radius on the QD is given by

$$\omega = \omega_0 + (L_{\text{LED}} + L_{\text{QD}}) * \tan \frac{\gamma}{2}, \tag{6}$$

where ω_0 is the beam waist radius.

Generally, to ensure the normal working of the QD, the spot is not allowed beyond the edge of the QD, as shown in Fig. 4. If the spot locates outside the QD, part of the beam will illuminate on the whole wall used to mount the QD and the scattering will generate. On the other hand, it introduces a relatively large position measurement error.[19] Thus, the spot radius arriving on the QD should satisfy the inequality below

$$d_{\text{QD}} + \omega \leq R_{\text{QD}}, \tag{7}$$

where R_{QD} is the radius of the QD. For the convenience of analysis, the L_{LED} and L_{QD} are conformed to the approximate relationship of $L_{\text{LED}} = L_{\text{QD}} = L$. Then, substituting Eqs. (3)–(5) into Eqs. (6) and (7), respectively, we can obtain

$$\begin{cases} 2L * \tan \frac{\gamma}{2} \geq \frac{L \tan(2\alpha) + b}{a} - \omega_0 \\ 2L * \tan \frac{\gamma}{2} \leq R_{\text{QD}} - \omega_0 - L \tan(2\alpha) \end{cases}, \tag{8}$$

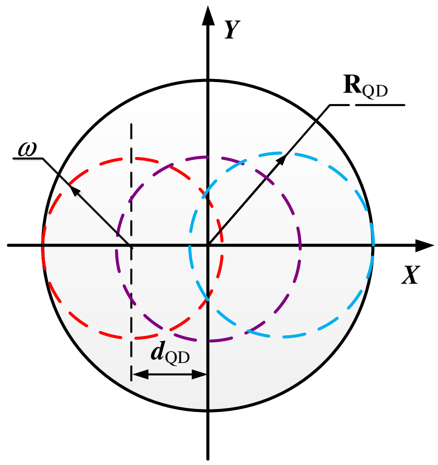

Fig. 4 The relationship between QD size and the range of spot moving.

where L is the half of the total optical path length. It is the mathematical model about the deflection angle, nonlinearity (a, b), divergence angle of LED, optical path length, and the radius of the QD. It is demonstrated that the large deflection angle and small nonlinearity are constrained with each other.

3.2 *Simulation and Analysis*

Utilizing the mathematical model above, we will discuss the effects of the optical path length and divergence angle on the deflection angle and linearity of FSM. A 7.8-mm-diameter QD is also used for the simulation and analysis below.

On the one hand, if the nonlinearity was 1%, the values of optical path length are 8 and 10 mm, respectively, the relation curves between the deflection angle and divergence angle are shown in Figs. 5(a) and 5(b). The black line is drawn according to the first inequation of Eq. (8), the red one is drawn based on the second inequation. The blue region is bounded by those two, which stands for the deflection angle and divergence angle, which are able to satisfy the 1% nonlinearity, and there are a largest deflection angle and the corresponding divergence angle in this area. Comparing Fig. 5(a) with Fig. 5(b), the obtained largest deflection angle is 2.5 deg corresponding to 22.5 deg divergence where the optical path length is 8 mm, whereas the largest deflection angle corresponding to the 18.1 deg divergence angle is 2.0 deg where the optical path length is 10 mm. Thus, the deflection angle decreases by about 0.5 deg and the corresponding divergence angle decreases by about 4.4 deg with the optical path length increasing by 2 mm.

By repeating the above process, changing the optical path length from 4 to 13 mm in the condition that the nonlinearity is also 1%, 10 couples of the largest deflection angle and corresponding divergence angle have been obtained and shown in Fig. 5(c). The largest deflection angle of the FSM reaches about 5 deg with 4-mm optical path length and divergence angle of 43 deg. It is illustrated that a larger deflection angle of FSM can be obtained as long as the DADS has a shorter optical path length and an LED has a larger divergence angle, when the nonlinearity of the QD is kept constant.

On the other hand, if the deflection angle is kept as 2 deg and the nonlinearities are 1%, 0.7%, and 0.5%, respectively,

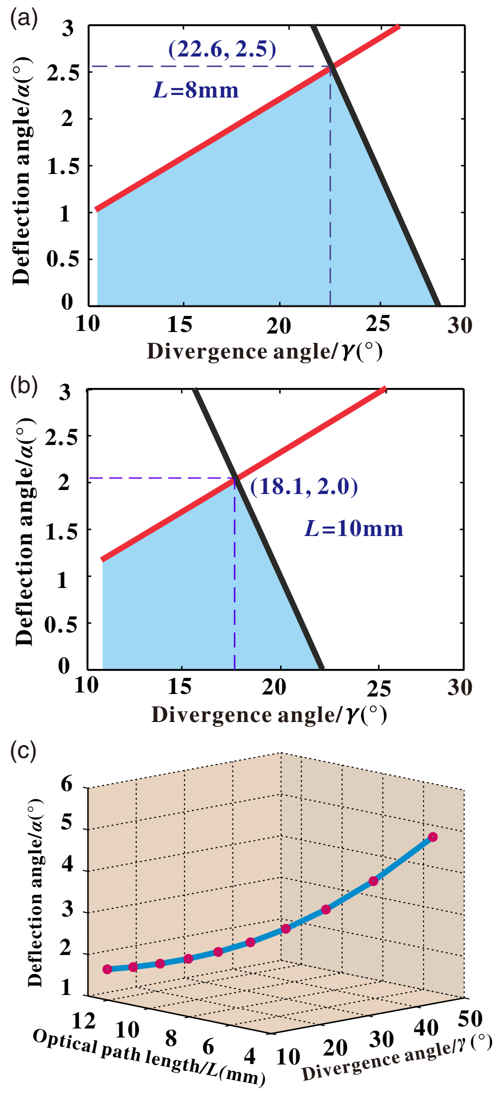

Fig. 5 The relationship between deflection angle and optical path length in (a) 8-mm optical path length and (b) 10-mm optical path length, the blue region shows the range of deflection angle corresponding to a certain divergence angle of the LED. (c) The relationship between the largest deflection angle, optical path length and divergence angle, optical path length varies from 4 to 13 mm.

the corresponding regions bounded by the divergence angle and optical path length can be acquired according to Eq. (8), as shown in Fig. 6. It can be easily seen that the first inequation depends on the nonlinearity parameters (a, b) and the three red curves correspond to the three values of nonlinearity above. However, the second inequation is independent on the nonlinearity, and it is described as the blue curve. It is illustrated that the region bounded by divergence angle and optical path length is $S_1 + S_2 + S_3$ when the nonlinearity of the QD is 1%, whereas its area is only S_1 when the nonlinearity of the QD is 0.5%. For the different nonlinearities, a maximum optical path length can be designed and an LED with minimum divergence angle length can be chosen. Therefore, it is illustrated that the nonlinearity is decreased with an increase in the optical path length when the divergence angle and the deflection angle are fixed.

According to the analysis of two aspects above, the method of seeking optimal deflection angle and linearity

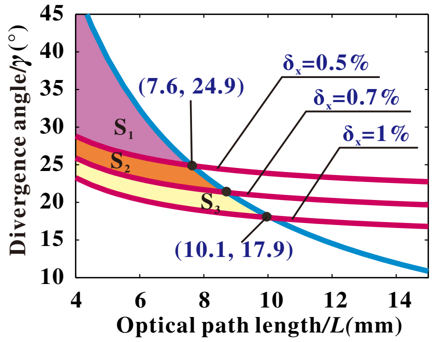

Fig. 6 The simulation results of the ranges of divergence angle and optical path length when the nonlinearity is different and deflection angle are kept constant.

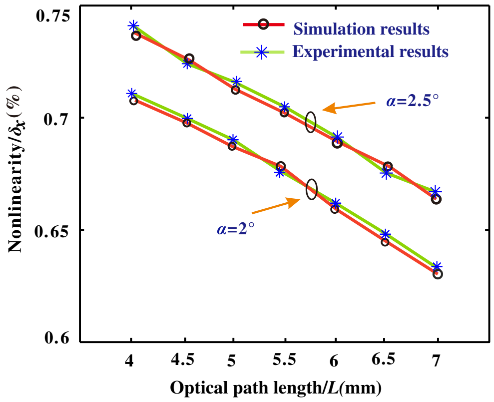

Fig. 8 The nonlinearity results of the DADS when the deflection angles are ±2 deg and ±2.5 deg, respectively. The red line describes the simulation nonlinearities. The green line describes the experimental nonlinearities.

of FSM has been expounded. By changing optical path length and divergence angle, the largest deflection angle can be obtained with one certain nonlinearity, and smaller nonlinearity can also be achieved with a certain deflection angle. Therefore, deflection angle and linearity of FSM can be optimized perfectly in this method. The method also can be extensively applied to the angle detecting system for active optical system and optical tweezers.[25,26]

4 Experiments and Results

4.1 *Experiment Setup of the Deflection Angle Detecting System*

As shown in Fig. 7, two 850-nm LEDs (OPTEK Technology OP296a and OP265a with the divergence angle of 25 deg and 20 deg, respectively) and a near-infrared QD (First Sensor Co., Ltd. QP50-6, 7.8-mm diameter and 0.042-mm gap) are used in this experiment. The QD and LED are mounted symmetrically about the mirror. The mirror is placed on the angle motion stage, which is used to adjust the deflection angle with the minimum moving step of 1 μrad; the LED is mounted on the five-dimensional position stage with the precision of 1 μm, and the QD is placed on the two-dimensional position stage with precision of 1 μm, those two position stage are used to adjust the optical path length. All the devices are mounted on an air-floating platform.

When the mirror is deflected, the output voltage generated on each quadrant can be collected by an analog-digital converter, then the deflection angle of the mirror can be calculated according to Eq. (1). In this experiment, the deflection angles of the angle motion stage are regarded as the theoretical values, and the measured angle by QD is regarded as experimental value. By comparing the theoretical deflection angle and the measured angle, we can calculate the nonlinearity based on the Eq. (2).

4.2 *Results and Analysis of the Deflection Angle Detecting System*

First, the 25 deg divergence angle LED is mounted on the five-dimensional position stage, the mirror is deflected

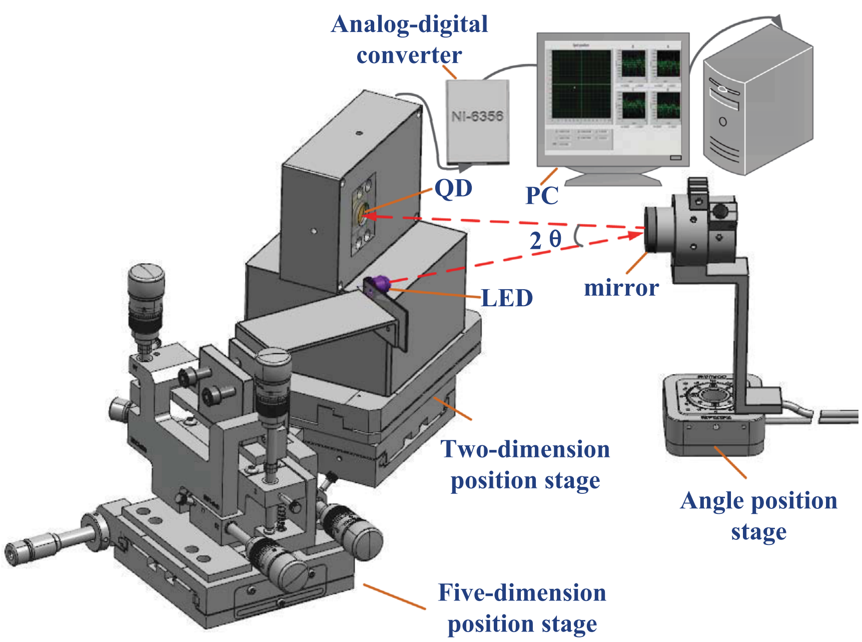

Fig. 7 The diagram of setup for the DADS.

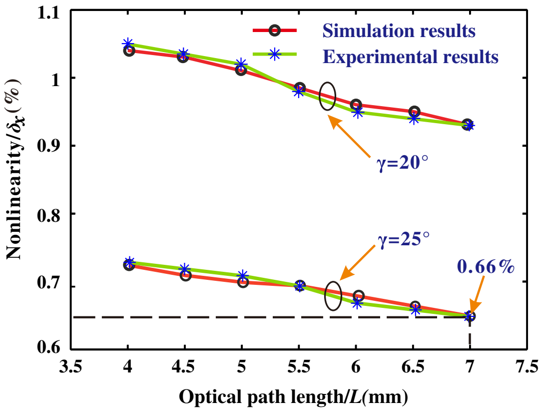

Fig. 9 The diagram of the nonlinearities of DADS using two LEDs (20 deg and 25 deg divergence angle). The red line represents the simulation results, the green line represents the experimental result.

from −2 deg to +2 deg in steps of 20 μrad, and optical path length is gradually changed from 4 to 7 mm in steps of 0.5 mm. The corresponding deflection angles can be measured by the QD. The mirror is rotated from −2.5 deg to +2.5 deg in steps of 20 μrad, and other conditions remain the same. Then, the simulation and experimental nonlinearities are shown in Fig. 8.

Figure 8 shows that the variations of experimental nonlinearity agree well with the simulation results when the deflection angles are ±2 deg and ±2.5 deg, respectively. It is also illustrated that the nonlinearity is decreased with the optical path length being enlarged, when the deflection angle and the LED are fixed. In addition, we can also obtain the smaller nonlinearity with ±2 deg deflection angle LED than ±2.5 deg under the same conditions. Meanwhile, the experimental results are affected by the mounting error caused by all the devices and the noise error caused by the LED and QD, respectively.

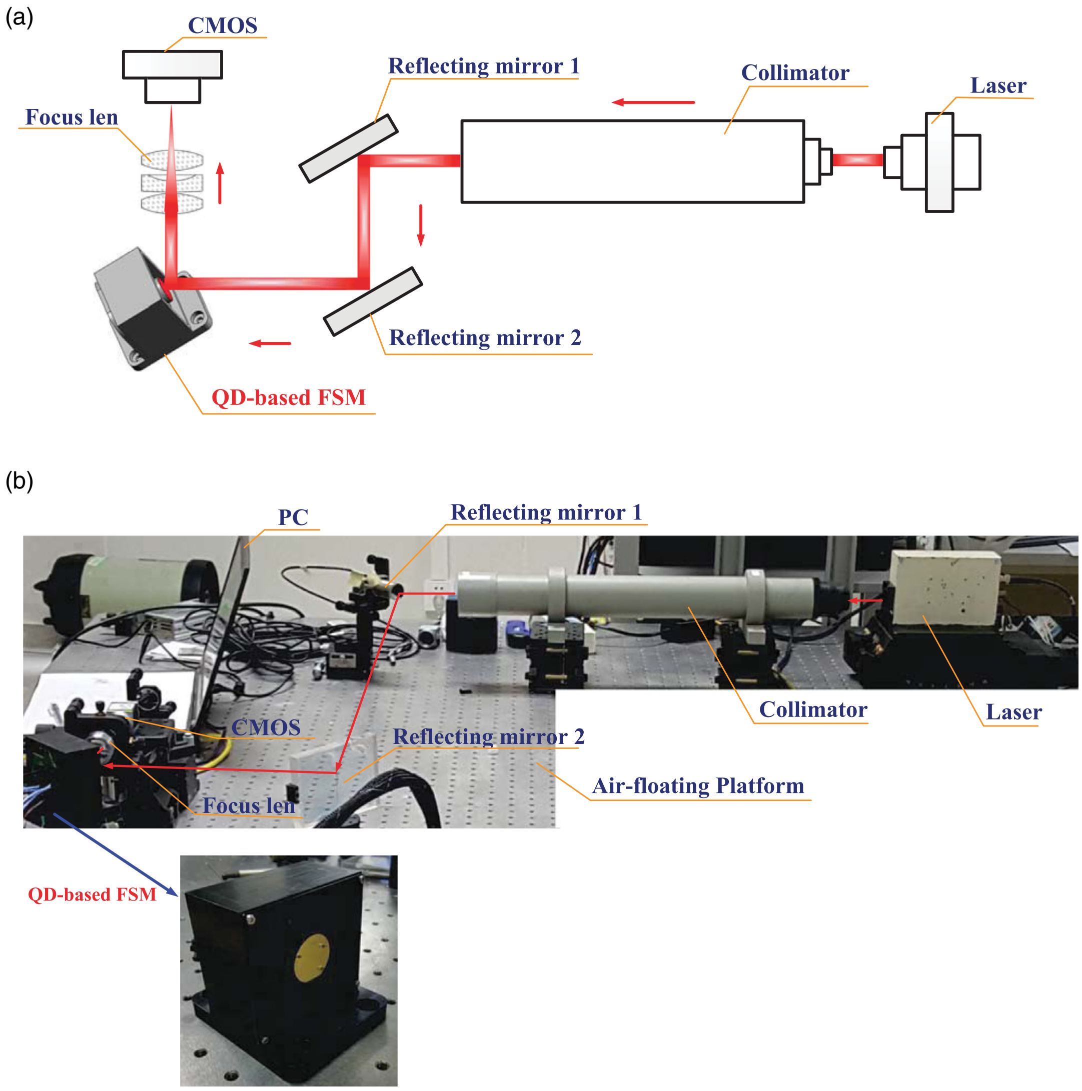

Fig. 10 (a) The experimental principle diagram of testing the deflection angle and linearity of the QD-based FSM. (b) The photograph of the testing platform for evaluating the linearity and deflection angle of the designed QD-based FSM.

Second, another 20 deg divergence angle LED is applied, and the mirror is also deflected from −2.5 deg to +2.5 deg. Figure 9 shows the experimental and simulation nonlinearities, which are obtained using two LEDs, respectively. It is also shown that the variations of the experimental nonlinearity agree well with the simulation results. In addition, the smaller nonlinearity is obtained using the 25 deg divergence angle LED than 20 deg. For example, when the optical path length is 4 mm, the obtained experimental 0.71% and 1.05% nonlinearities, respectively, correspond to the 25 deg and 20 deg divergence angle LED.

Finally, based on the simulation results, we design the DADS with 7-mm optical path length, 25 deg divergence angle LED 10-mm-diameter minor mirror for FSM to improve the deflection angle and linearity. Based on the experimental results, it achieves 0.62% nonlinearity.

In summary, the mathematical model [Eq. (8)] is proved correct and feasible in QD-based FSM using simulation and experimental results since the experimental results agree well with the simulation results. Therefore, this optimization method provides an efficient project to design the DADS for QD-based FSM.

4.3 *Experimental Setup of the Designed Quadrant Detector-Based Fast Steering Mirror*

On the basis of analyzing the experimental results of the DADS, the 25 deg divergence angle LED and the QD are chosen to design it for achieving higher linearity. Its optical path length is fixed to 7 mm. The 10-mm-diameter minor mirror, the 25-mm-diameter major mirror, and the 4 VCAs (Akribis AVM 14-10-C56) are assembled on the QD-based FSM. To evaluate the linearity of the FSM within the deflection angle range, we set up the test platform, as shown in Fig. 10. The experimental principle of testing the deflection angle and linearity of the QD-based FSM and the test platform are shown in Figs. 10(a) and 10(b), respectively.

The mirror of the FSM can be driven by the VCAs to deflect a corresponding mirror when a certain drive voltage is input. The spot is moving on the surface of the camera if the FSM is deflected a certain angle, so the deflection angle range of the FSM can be measured according to the spot displacement on the surface of the camera.

4.4 *Results and Analysis of the Designed Quadrant Detector-Based Fast Steering Mirror*

We obtain a group of corresponding deflection angles when the FSM is driven to deflect a series of angles. Based on these data, the relations curve between the deflection angle and the drive voltage are shown in Figs. 11(a) and 11(b). The nonlinearity is 0.72% within the deflection angle range of ±2.0 deg in the x-axis, the nonlinearity is 0.68% within the deflection angle range of ±2.0 deg in the y-axis, respectively. However, the experimental nonlinearity of the independent DADS is about 0.66% within the ±2.0 deg deflection angle in x-axis, as shown in Fig. 9. Those main reasons for increasing the nonlinearity of the FSM are in the following aspects: mounting errors of the DADS, rotation errors of the flexible hinge support, and moving errors of the VCA, etc. So, we will continue to focus on decreasing the nonlinearity of the FSM by optimizing the DADS and changing the energy distribution of the LED.

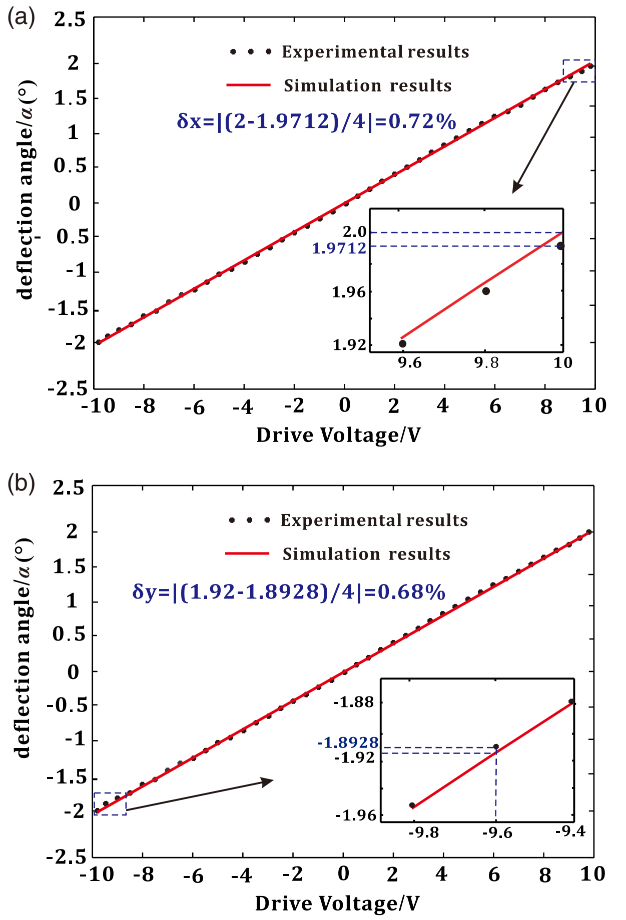

Fig. 11 (a) Experimental and simulation results of deflection angle and nonlinearity of the designed QD-based FSM in the x-axis; (b) Experimental and simulation results of deflection angle and nonlinearity of the designed QD-based FSM in the y-axis. The insert shows the biggest position error within the whole deflection angle range, the black spots represent the experimental results, the red line represents simulation results, δ is the nonlinearity of the designed QD-based FSM.

Moreover, we also test the resolution of the QD-based FSM. We employ the 16-bit AD converter and 16-bit DA converter. The resolution of the FSM is 1.047 μrad if the noise is not considered. The FSM is, respectively, deflected at (0, 0), (210 μrad, 210 μrad), and (2100 μrad, 2100 μrad), we collect 2500 position changing data, which detected by the QD, respectively. Then, we calculate the root-mean-square value of the position changing data (RMS), which is the resolution of the FSM. The results are shown in Fig. 12;, it shows that the resolutions (RMS) are 1.11, 1.3, and 1.6 μrad when the FSM is deflected at (0, 0), (210 μrad, 210 μrad), and (2100 μrad, 2100 μrad), respectively. So, the minimum resolution appears when the FSM mirror is in the position of (0, 0). The resolution becomes worse with enlarging the deflection angle of the FSM.

Researchers have done a lot of studies about the FSMs. There are several kinds of FSMs that are shown in Table 2. Our designed FSM achieves 2.5 deg deflection angle, 0.72% nonlinearity, and 1.11-μrad resolution. Compared with FSM in Ref. 8 (which has ±1.125 deg and ±2.5 deg deflection angle in the x-axis and y-axis, respectively, 2.67% nonlinearity and 50-μrad resolution), the nonlinearity, deflection

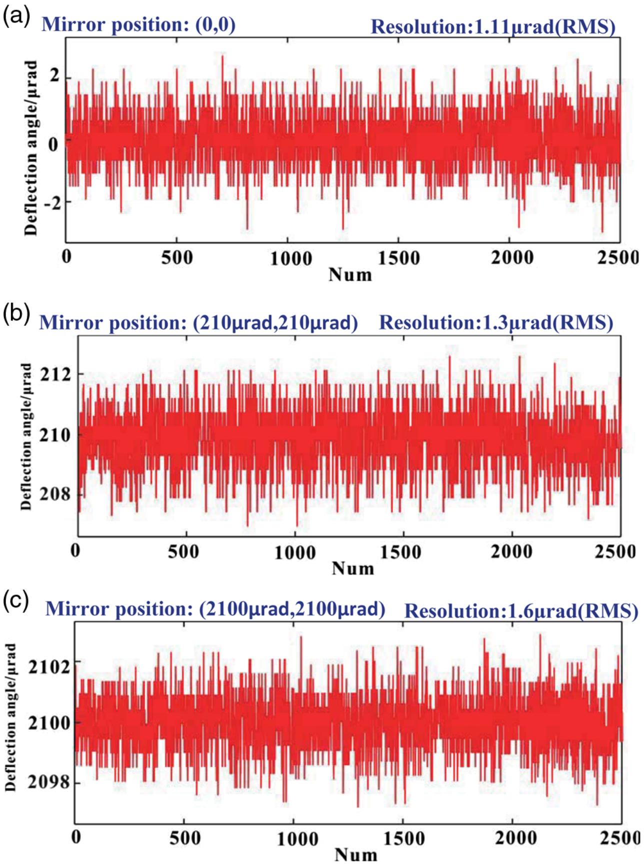

Fig. 12 The experimental resolutions of the QD-based FSM when the FSM mirror is in different positions. (a) the mirror is at the position of (0, 0), (b) the mirror is at the position of ($210\ \mu$rad, $210\ \mu$rad), and (c) the mirror is at the position of ($2100\ \mu$rad, $2100\ \mu$rad).

Table 2 Parameters of several kinds of FSMs.

FSMs	Deflection angle	Nonlinearity	Resolution (RMS) (μrad)
Ref. 8	± 1.125 deg / ± 2.5 deg (along x/y axis)	2.67%	50
Ref. 13	± 1.5 deg (along two axes)	1%	1
Ref. 14	± 5 deg (along two axes)		9.7
This paper	± 2.0 deg (along two axes)	0.72%	1.11

angle, and resolution in the x-axis of our QD-based are much better than that of Ref. 8. In comparison with the FSM in Ref. 13 (which achieves ± 1.5 deg deflection angle, 1% nonlinearity, and 1-μrad resolution), the deflection angle and nonlinearity of our FSM are both better than that of Ref. 13, respectively, the resolution is decreased by 10%. The deflection angle of our FSM is 24 times as large as that in Ref. 14 (which obtains ± 5 deg deflection angle and 9.7-μrad resolution), and the resolution of our FSM is 1.11 μrad. In addition, the measurement range of the DADS can be further increased by changing the design scheme (including changing the divergence angle of the LED, optical path length or adding the lens), which will be our focus in the future work. Therefore, this QD-based FSM is very helpful for improving the precision and extend the acquisition field of the APT in FSO system.

5 Conclusion

The DADS using the QD for FSM has been studied in detail in this paper. Its mathematical model has been established by analyzing the principle of position detecting and error characteristics of the QD. On the basis of this mathematical model, the method of optimizing the deflection angle and the linearity has been expounded. The simulation and the experimental results have proved the mathematical model correct and valuable for designing QD-based FSM. Finally, we assemble the QD-based FSM and establish test platform to evaluate its performances. The results show that the designed QD-based FSM achieves 0.72% nonlinearity, ± 2.0 deg deflection angle, 1.11-μrad resolution, and 700 Hz. Comparing the performances with other FSMs shows that the QD-based FSM achieves larger deflection angle and better linearity simultaneously. Therefore, this method of optimizing the DADS will be beneficial to design the large deflection angle and high linearity FSM.

Acknowledgments

The authors thank Qiang Lu and Yue Wang for discussions about this paper. National Natural Science Foundation of China (NSFC) (51605465).

References

1. K. P. Peppas and P. T. Mathiopoulos, "Free-space optical communication with spatial modulation and coherent detection over H–K atmospheric turbulence channels," *J. Lightwave Technol.* **33**, 4221–4232 (2015).
2. X. M. Zhu and J. M. Kahn, "Free-space optical communication through atmospheric turbulence channels," *IEEE Trans. Commun.* **50**, 1293–1300 (2002).
3. M. R. Suite et al., "Fast steering mirror implementation for reduction of focal-spot wander in a long-distance free-space communication link," *Proc. SPIE* **5160**, 439–446 (2004).
4. D. J. Kluk, M. T. Boulet, and D. L. Trumper, "A high-bandwidth, high-precision, two-axis steering mirror with moving iron actuator," *Mechatronics* **22**, 257–270 (2012).
5. C. S. Sun et al., "Backscanning step and stare imaging system with high frame rate and wide coverage," *Appl. Opt.* **54**, 4960–4965 (2015).
6. T. Weyrauch and M. A. Vorontsov, "Atmospheric compensation with a speckle beacon in strong scintillation conditions: directed energy and laser communication applications," *Appl. Opt.* **44**, 6388–6401 (2005).
7. T. Tang et al., "Acceleration feedback of a CCD-based tracking loop for fast steering mirror," *Opt. Eng.* **48**(1), 013001 (2009).
8. X. Wu, S. H. Chen, and W. Chen, "Large angle and high linearity two-dimensional laser scanner based on voice coil actuators," *Rev. Sci. Instrum.* **82**, 105103 (2011).
9. B. U. Nam et al., "Design and analysis of a tip-tilt guide mechanism for the fast steering of a large-scale mirror," *Opt. Eng.* **55**(10), 106120 (2016).
10. Y. J. Long et al., "Modeling and design of a normal stress electromagnetic actuator with linear characteristics for fast steering mirror," *Opt. Eng.* **53**(5), 054102 (2014).
11. M. W. Fan et al., "A fast high voltage driver for the piezoelectric fast steering mirror," *Proc. SPIE* **9255**, 925539 (2015).
12. X. H. Zhai et al., "The optimized structure design in improving the bandwidth of fast steering mirror," *Proc. SPIE* **8906**, 89060J (2013).
13. OIM101-One Inch FSM, http://www.opticsinmotion.net/OIM101%20INFO%20Update%2010-08-10.pdf.
14. Y. F. Lu, "Research on fast/fine steering mirror system," PhD Thesis, p. 76, Graduate School of National University of Defense Technology (2009).
15. A. Berta et al., "Development of a commercial line of high-performance, fast-steering mirrors," *Proc. SPIE* **3787**, 181–192 (1999).
16. W. B. Dobie, P. C. G. Isaac, and G. O. Gale, "Electrical resistance strain gauge," *Am. J. Phys.* **18**, 117–118 (1950).
17. J. Zhang et al., "Advanced in InGaAs/InP single-photon detector system for quantum communication," *Light* **4**, e286 (2015).
18. S. Cui and Y. C. Soh, "Improved measurement accuracy of the quadrant detector through improvement of linearity index," *Appl. Phys. Lett.* **96**, 081102 (2010).

19. M. W. Chen, Y. P. Yang, and X. T. Jia, "Investigation of position algorithm and method for increasing the linear measurement range for four-quadrant detector," *Optik* **124**, 6806–6809 (2013).
20. Q. K. Zhou et al., "Design of fast steering mirror system for precision laser beam steering," in *IEEE Int. Workshop on Robotic and Sensors Environments* (2008).
21. A. J. Makynen, J. T. Kostamovaara, and R. A. Myllyla, "Position sensitive detection techniques for manufacturing accuracy control," *Proc. SPIE* **1194**, 243–252 (1989).
22. L. M. Manojlovic, "Quadrant photodetector sensitivity," *Appl. Opt.* **50**, 3461–3469 (2011).
23. L. H. Zhang et al., "Linearity of quadrant avalanche photodiode in laser tracking system," *Chin. Opt. Lett.* **7**(8), 728–731 (2009).
24. J. Narag and N. Hermosa, "Response of quadrant detectors to structured beams via convolution integrals," *J. Opt. Soc. Am. A* **34**(7), 1212–1216 (2017).
25. X. D. Tao, H. Cho, and J. S. Farrokh, "Active optical system for variable view imaging of micro objects with emphasis on kinematic analysis," *Appl. Opt.* **47**, 4121–4131 (2008).
26. J. H. G. Huisstede et al., "Force detection in optical tweezers using backscattered light," *Opt. Express* **13**, 1113–1123 (2005).

Yingxue Ni received her BS degree in mechanical electrical engineering from Changchun Institute of Technology, China. Currently, she is working toward her PhD in mechanical manufacturing and automation at University of Chinese Academy of Sciences, China. Her current research interests include optics, fine mechanical control, and space optical communication.

Jiabin Wu joined the Laser Communication team in 2016 after earning his PhD in mechanical electronic engineering from the University of Chinese Academy of Sciences, China. He is studying space laser communications and FSM at present.

Xiaogang San received his PhD in mechanical electronic engineering from the University of Chinese Academy of Sciences, China. Currently, he researches Laser Communication in CIOMP, China. He is occupied in design of the photoelectrical automatic target-scoring system.

Shijie Gao organized the Laser Communication team in CIOMP in 2014. He received his PhD in mechanical electronic engineering from the University of Chinese Academy of Sciences, China, in 2015.

Shaohang Ding is one of the researchers of the Laser Communication team in CIOMP, China. Currently, He is working toward his PhD in mechanical manufacturing and automation at University of Chinese Academy of Sciences, China.

Jing Wang is a professor and doctoral supervisor in CIOMP, China. She is mainly engaged in the research of photoelectric imaging and measurement technology. A number of heavy caliber and high precision theodolites have been completed under her guidance.

Tao Wang received his BS degree from Shanghai Jiao Tong University, China. Currently, he is working toward his PhD in mechanical manufacturing and automation at University of Chinese Academy of Sciences, China.